4988 *Biochemistry* **2009,** *48,* 4988–4998
DOI: 10.1021/bi9002343

BIOCHEMISTRY
including biophysical chemistry & molecular biology
Article

Flexibility in the Inducer Binding Region Is Crucial for Allostery in the *Escherichia coli* Lactose Repressor[†]

Jia Xu*[,‡] and Kathleen S. Matthews[‡,§]

[‡]*Department of Biochemistry and Cell Biology and* [§]*W. M. Keck Center for Interdisciplinary Bioscience Training, Rice University, 6100 South Main Street, Houston, Texas 77005*

Received February 12, 2009; Revised Manuscript Received April 10, 2009

ABSTRACT: Lactose repressor protein (LacI) utilizes an allosteric mechanism to regulate transcription in *Escherichia coli*, and the transition between inducer- and operator-bound states has been simulated by targeted molecular dynamics (TMD). The side chains of amino acids 149 and 193 interact and were predicted by TMD simulation to play a critical role in the early stages of the LacI conformational change. D149 contacts IPTG directly, and variations at this site provide the opportunity to dissect its role in inducer binding and signal transduction. Single mutants at D149 or S193 exhibit a minimal change in operator binding, and alterations in inducer binding parallel changes in operator release, indicating normal allosteric response. The observation that the double mutant D149A/S193A exhibits wild-type properties excludes the requirement for inter-residue hydrogen bond formation in the allosteric response. The double mutant D149C/S193C purified from cell extracts shows decreased sensitivity to inducer binding while retaining wild-type binding affinities and kinetic constants for both operator and inducer. By manipulating cysteine oxidation, we show that the more reduced state of D149C/S193C responds to inducer more like the wild-type protein, whereas the more oxidized state displays diminished inducer sensitivity. These features of D149C/S193C indicate that the novel disulfide bond formed in this mutant impedes the allosteric transition, consistent with the role of this region predicted by TMD simulation. Together, these results establish the requirement for flexibility in the spatial relationship between D149 and S193 rather than a specific D149−S193 interaction in the LacI allosteric response to inducer.

Allosteric regulation is a major mechanism of control in many biological processes, including cell signaling as well as genetic and metabolic regulation (*1*, *2*). Although allosteric behavior is a common feature for many regulatory proteins, a detailed atomic-level description of this mechanism remains largely elusive. Lactose repressor protein (LacI)[1] is a prototypic genetic regulatory protein that regulates transcription of the *lac* operon genes (*3*), which encode enzymes responsible for metabolism of lactose in *Escherichia coli* (*3*, *4*). High-affinity binding of repressor to operator sequences within the *lac* operon (*5*) precludes transcription of the *lac* metabolic enzymes by RNA polymerase (*4*). Diminished affinity for the target operator DNA and a consequent increase in the level of *lac* mRNA transcription result from a conformational change in response to binding a metabolite of lactose (1,6-allolactose) to a site within LacI distant from the DNA site (*4*).

LacI is a well-characterized tetrameric protein comprised of identical monomers. The structure of the monomer can be dissected into three major elements (Figure 1A,B): an N-terminal DNA binding domain (amino acids 1−60), a core domain (amino acids 61−330) that binds inducer and forms the dimer interface, and a C-terminal domain (amino acids 331−360) that generates the tetramer interface (*6*−*9*). The core domain of LacI is structurally homologous with the venus fly trap (VFT) family that includes bacterial periplasmic binding proteins (PBPs) involved in transport and the extracellular domain of G-protein-coupled receptors (GPCRs) as well as other receptors that transduce extracellular stimuli into intracellular signals and exhibit subdomain movements associated with function (*10*−*12*). In this larger functional context, significant efforts have been made to study allosteric behavior in LacI, which brings enormous biochemical and structural information to facilitate more detailed analysis (*4*, *8*, *13*−*17*).

The three-dimensional structures of the core domain and full-length LacI in both operator- and IPTG-bound conformations are available (*7*, *8*, *16*). The shift in LacI structure between operator- and inducer-bound conformations requires both rotation and translation of the N-subdomain within the core domain (Figure 1B) (*8*, *16*). Amino acids D149 and S193 are located near the IPTG binding pocket at the interface of the N- and C-subdomains (Figure 1A). Shifts in the side chains at D149

[†]This work was supported by grants from the Robert A. Welch Foundation (C-576) and the National Institutes of Health (GM22441) to K.S.M.

*To whom correspondence should be addressed. Telephone: (713) 348-4936. Fax: (713) 348-6149. E-mail: jiaxu@rice.edu.

[1]Abbreviations: DTNB, dithionitrobenzoic acid; DTT, dithiothreitol; IPTG, isopropyl β-D-thiogalactoside; LacI, lactose repressor protein; PDB, Protein Data Bank; TMD, targeted molecular dynamics; WT, wild-type.

Published on Web 04/15/2009

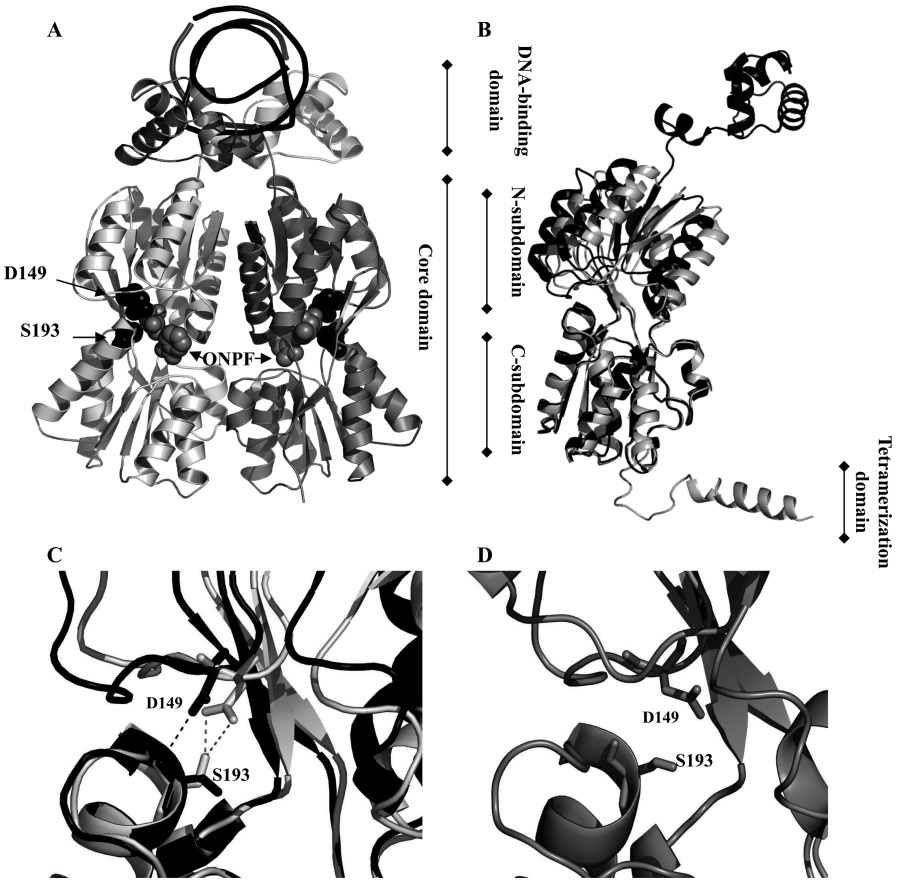

FIGURE 1: (A) Structure for dimeric LacI bound to O^{sym} DNA (top, black) and anti-inducer ONPF (gray space-filling diagram) with positions 149 and 193 highlighted in black space-filling diagrams (dimer variant from PDB entry 1efa) (*16*). The two monomers are displayed in distinct colors (light gray and dark gray). (B) The monomer from 1efa (black) (*16*) and the monomer from 1lbh (gray) (*8*) were aligned using residues in the core C-subdomain. Note the changes in the N-subdomains. (C) Detailed view of D149 and S193 in the O_{sym}·ONPF·LacI structure (1efa, black) (*16*) and the IPTG·LacI structure (1lbh, gray) (*8*). Residues 149 and 193 are highlighted by sticks, and hydrogen bonds are shown as dashed lines. Note the movement of the backbone surrounding D149 and the altered positions of the side chains of D149 and S193 in these two conformations. (D) Intermediate state simulated by TMD (*18*). Notice that the side chain of residue 149 is in a position different from those of both IPTG-bound and DNA-bound states.

and S193 as well as substantial movement of the backbone of D149 are observed between DNA- and IPTG-bound LacI structures (Figure 1C). D149 occupies a key position at the start of a flexible loop that comprises residues from position 149 to 156. In the DNA-bound structure, a single bond is formed between the backbone of S193 and the side chain of D149; however, in the IPTG-bound structure, the D149 side chain forms two hydrogen bonds to the S193 side chain in each monomer (Figure 1C) (*8*, *16*). This alteration suggests D149 and S193 might be participants in determining the distinct conformational states of the repressor.

Recently, a TMD simulation was utilized to simulate the conformational transition pathways in LacI (*18*). This prediction for the operator-bound to IPTG-bound forms shows significant movement in the flexible loop containing D149 at early stages of the conformational change. Mobility in this flexible loop allows the side chain of residue 149 to move ~4 Å, forming hydrogen bonds with the side chain at position 193. These hydrogen bonds may secure the flexible loop in place (*18*). This event appears to be critical in the initial stages of propagating the message of inducer binding through the N-subdomain of LacI to the DNA binding domain. In the intermediate state of TMD simulation (Figure 1D) (*18*), the side chain of residue 149 points to a position close to neither the IPTG-bound state nor the DNA-bound state. This observation further supports the hypothesis that the region around residue 149 contributes to transmittance of the allosteric signal. Consistent with their predicted importance, alterations at positions 149 and 193 resulted in a diminished response to IPTG binding in phenotypic screens (*14*). Further, because D149 is among the residues that directly contact inducer IPTG, exploring this region provides an opportunity to examine whether IPTG binding and signal transduction capacities can be uncoupled. To dissect the structural and functional influence of this specific region, multiple single substitutions at positions 149 or 193 were examined. Double substitutions, D149A/S193A and D149C/S193C, were introduced, and their biochemical and biophysical characteristics were examined to explore the role of specific side chain interaction and flexibility of the region in the LacI allosteric response.

MATERIALS AND METHODS

Site-Specific Mutagenesis and Purification. Plasmid pJC1 (*9*) containing the complete LacI gene was used as the expression vector in *E. coli* BLIM cells (*19*). All substitutions were derived by site-directed mutagenesis (Quickchange, Stratagene Inc.) using the corresponding oligonucleotides. Full sequencing of each LacI gene (SeqWright Inc.) verified the presence of only the expected mutation. For protein expression, cells transformed with specific plasmids were grown in 2× YT liquid medium in a shaking incubator at 37 °C for ~20 h. The cells were centrifuged and

resuspended in breaking buffer [0.2 M Tris-HCl (pH 7.6), 0.2 M KCl, 0.01 M magnesium acetate, 5% glucose, 0.3 mM DTT, and 0.3 μM PMSF] containing lysozyme and frozen at −20 °C. The frozen cells were slowly thawed and treated with 80 μL of 10 mg/mL DNaseI and $MgCl_2$ (final concentration of 10 mM). Following centrifugation, the supernatant was mixed with ammonium sulfate to a final level of saturation of 37% and centrifuged, and the resuspended pellet was dialyzed overnight against 0.09 M KP buffer [0.09 M potassium phosphate (pH 7.6), 0.3 mM DTT, and 5% glucose] at 4 °C. After the removal of any precipitate by centrifugation, the supernatant was applied to a phosphocellulose column equilibrated in 0.09 M KP buffer and eluted with a gradient from 0.12 to 0.30 M KP buffer [0.12−0.30 M potassium phosphate (pH 7.6), 0.3 mM DTT, and 5% glucose]. Protein purity was assessed by using SDS−PAGE and was ≥90%. Stoichiometric DNA binding activity for each repressor variant was determined by a filter binding assay described in the following section. Activities for purified proteins were ≥90%.

Operator Binding. DNA binding experiments were performed via a nitrocellulose filter binding assay (*20*, *21*) with a 40 bp natural operator (5′-TGTTGTGTGGAATTGTGAGCGGATAACAATTTCACACAGG-3′) (Biosource International). This assay was carried out in FB buffer [0.01 M Tris-HCl (pH 7.4), 0.15 M KCl, 0.1 mM DTT, 0.1 mM EDTA, and 5% DMSO] with 100 μg/mL bovine serum albumin. Protein at various dilutions (1×10^{-13} to 5×10^{-9} M) was first mixed with ^{32}P-labeled DNA. To determine DNA activity under stoichiometric conditions, the percentage of active repressor was measured with a DNA concentration at least 10-fold above the K_d. To measure DNA binding affinity, the DNA concentration was set at least 10-fold below the K_d. After a short incubation, the mixtures were filtered through nitrocellulose using a 96-well plate and exposed to a Fuji phosphorimaging plate overnight. The plate was read by a Fuji phosphorimager, and the radioactivity was quantified and analyzed with Igor Pro (Wavemetrics) to determine the binding affinity with the following equation:

$$Y_{obs} = Y_{max}\frac{[\text{Protein}]^n}{K_d{}^n + [\text{Protein}]^n} + c \quad (1)$$

where Y_{obs} is the observed level of retained radioactivity at a given protein concentration, Y_{max} is the level of radioactivity measured at saturation, c is the background radioactivity detected when no repressor is present, and K_d is the equilibrium dissociation constant. The value of the Hill coefficient, n, is generally ∼1 for LacI.

IPTG Binding. IPTG binding to repressor proteins was monitored by the fluorescence emission shift for intrinsic tryptophan that has been shown to accompany IPTG binding (*22*). The protein solution was placed in a 1 cm^2 quartz cuvette at room temperature, and the fluorescence emission intensity change at >350 nm was monitored at varying IPTG concentrations (*22*). The protein concentration was fixed at $\sim 1.5 \times 10^{-7}$ M monomer in fluorescence buffer containing 0.01 M Tris-HCl and 0.15 M KCl (pH 7.4), and the IPTG concentration was in the range of 1×10^{-8} to 1×10^{-3} M. The experiment was performed using an SLM-Aminco AB2 spectrofluorometer with an excitation wavelength of 285 nm. The emission spectra were recorded between 300 and 380 nm. The binding affinity for the protein was determined by fitting the data in Igor Pro using eq 2

$$Y_{obs} = Y_{max} - Y_{max}\frac{[\text{IPTG}]^n}{K_d{}^n + [\text{IPTG}]^n} + c \quad (2)$$

where K_d is the equilibrium dissociation constant, Y_{obs} is the measured fluoresence at a given IPTG concentration, Y_{max} is the maximum change in fluorescence signal between zero and saturating inducer, c is a constant background coefficient, and n is the Hill coefficient, which is ∼1 in the absence of the operator.

Operator Release. The operator release assay measures the effect of inducer sugar on DNA binding affinity (*23*). IPTG ranging from 10^{-8} to 10^{-3} M was added following mixture of the protein and labeled operator DNA in FB buffer with 100 μg/mL bovine serum albumin. After incubation for ∼30 min, nitrocellulose filter binding was used to monitor the level of DNA bound in the presence of varied inducer concentrations. The concentration of DNA was at least 10-fold below the K_d obtained from the operator binding assay ($\sim 10^{-12}$ M), and the concentration of protein was set to ∼80% of the maximal DNA binding for the specific repressor protein. Data were analyzed with Igor Pro using a variation of eq 2. In this case, K_d is substituted with $[\text{IPTG}]_{mid}$, corresponding to the concentration of IPTG required to release 50% of the protein−DNA complex. Y_{obs} is the measured radioactivity at a specific inducer concentration; Y_{max} is the maximum radioactivity differential observed, and c is the radioactivity with no protein present.

Kinetic Measurements of Repressor−IPTG Association. The association rates for IPTG binding to LacI were measured using a stopped-flow system equipped with fluorescence detection (Applied Photophysics Ltd.) (*24*). The association processes were monitored as the fluorescence decrease due to IPTG binding. The excitation wavelength was 285 nm, and fluorescence emission was monitored using a 350 nm cutoff filter. Time courses were measured for the association of repressor with IPTG under pseudo-first-order conditions. The final LacI concentration was 1.0×10^{-6} M, and IPTG concentrations were varied from 0.05 to 0.2 mM in buffer containing 0.01 M Tris-HCl (pH 7.4) and 0.15 M KCl. The association rate constants were determined by fitting observed rate constant (k_{obs}) using the equation

$$k_{obs} = k_{assoc}[\text{IPTG}] + k_{dissoc} \quad (3)$$

where k_{assoc} and k_{dissoc} are the association and dissociation rate constants, respectively.

Kinetic Measurements of Repressor−Operator Dissociation. Operator dissociation rate analysis utilized the nitrocellulose binding assay (*25*). LacI (1.8×10^{-11} M) and ^{32}P-labeled DNA (3.6×10^{-11} M) in a total volume of 10 mL were equilibrated for 15 min at room temperature in FB buffer containing 0.01 M Tris-HCl (pH 7.4), 0.15 M KCl, 0.1 mM EDTA, and 5% DMSO with 100 μg/mL bovine serum albumin. An excess of unlabeled DNA over the initial DNA concentration (90-fold excess) was added to the equilibrated solution, immediately followed by gentle inversion of the tube three times. Duplicate aliquots (100 μL) were withdrawn and filtered on a nitrocellulose membrane at the desired times. Reactions were monitored until equilibrium was reached at ∼2 h. The equilibrium value, corresponding to background retention of DNA, was subtracted from each time point. The dissociation rate constant was determined by fitting the data to a single-exponential model.

Formation of Oxidized- and Reduced-State Protein. The oxidized state of the double-cysteine mutant was obtained by

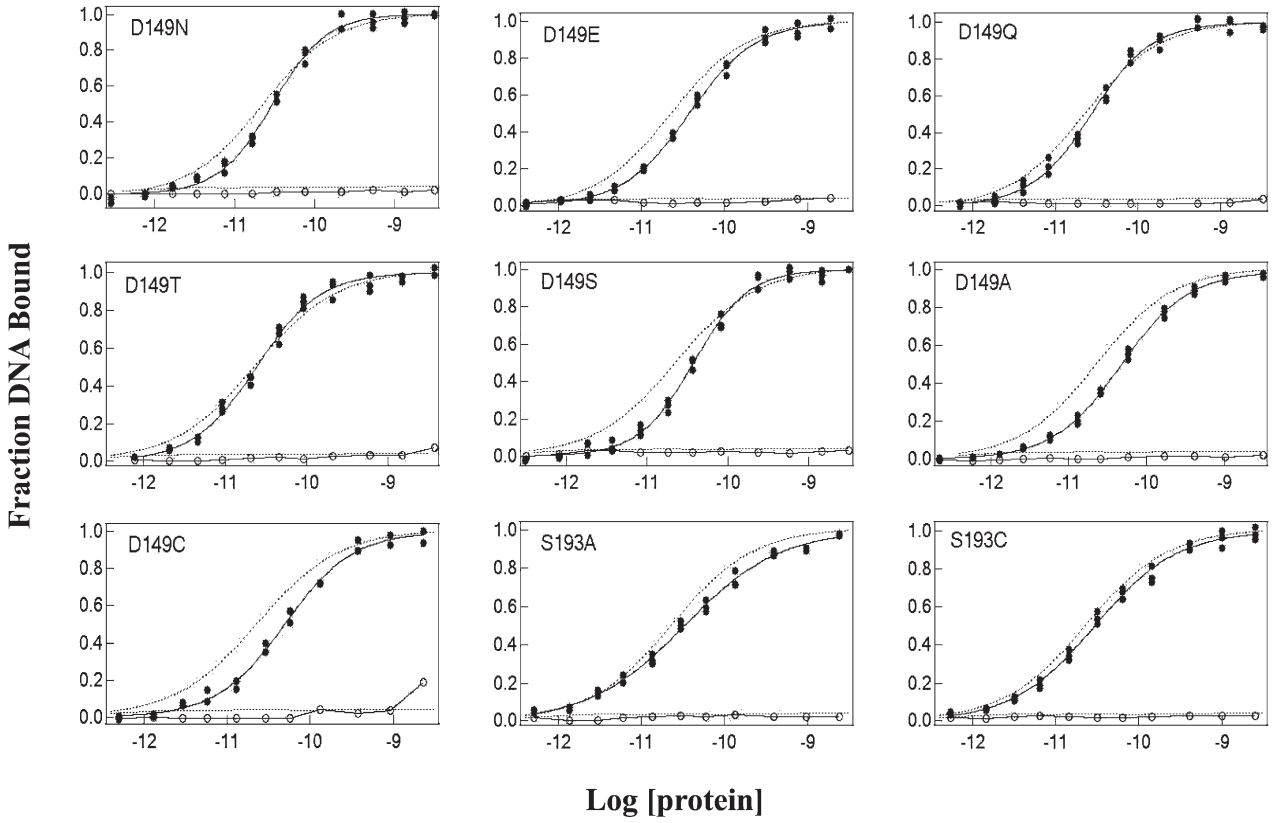

FIGURE 2: Operator binding curves for wild-type LacI and single mutants. Wild-type LacI binding is represented by the dotted line in each panel for the sake of comparison. Equilibrium dissociation constants were determined by a filter binding assay as described in Materials and Methods. Protein (1×10^{-13} to 5×10^{-9} M) and operator DNA ($\sim 1.5 \times 10^{-12}$ M) were in FB buffer [0.01 M Tris-HCl (pH 7.4), 0.15 M KCl, 0.1 mM EDTA, and 5% DMSO] with 100 μg/mL bovine serum albumin. The fraction of DNA bound in the absence of IPTG is shown as filled circles and in the presence of 1 mM IPTG as empty circles. The curves shown were generated by fitting the data using Igor Pro. Results from multiple experiments are listed in Table 1.

utilizing a Hitrap desalting column (GE Healthcare Corp.) to remove DTT from the protein solution. After elution from the column, the solution was dialyzed in air-purged fluorescence buffer [0.01 M Tris-HCl and 0.15 M KCl (pH 7.4)] for ~1 h to further enhance the oxidized state. The corresponding reduced-state measurement was achieved by exposure of the protein to a high concentration of DTT and 6 M urea followed by rapid elution through a Hitrap desalting column using fluorescence buffer to remove excess DTT.

Chemical Modification. Ellman's reagent, 5,5′-dithiobis (2-nitrobenzoic acid) (DTNB), was used to determine the free sulfhydryl content in LacI (*26*, *27*). A volume of 100 μL of the denatured protein sample (with a final monomer concentration in the range of ~1−10 μM in the presence of 6 M urea) was added to 50 μL of reaction buffer [0.1 M sodium phosphate (pH 7.6) and 1 mM EDTA] and 20 μL of Ellman's reagent. To measure the background, 100 μL of reaction buffer was utilized instead of a protein solution. After incubation at room temperature to complete the reaction (~15 min), the absorbance at 412 nm was determined against buffer background to quantify the amount of product released from the reaction between an active thiolate of protein cysteines and DTNB using an extinction coefficient (ε) of 14290 cm^{-1} M^{-1}.

RESULTS

Single Mutations at D149 and S193. We generated a series of single substitutions for D149 to explore the functional impact of alterations in electrostatics, polarity, size, hydrogen bonding capacity, and hydrophobic character. For operator binding affinity, D149 and S193 single mutants display values within ~2-fold of those of wild-type LacI in the absence of IPTG (Figure 2 and Table 1). In the presence of 1 mM IPTG, all the single mutants have sensitivity to IPTG binding similar to that of wild-type LacI, with the possible exception of D149C (Figure 2 and Table 1). For IPTG binding, substitutions with N, S, and A at residue D149 decreased binding affinity only slightly. The affinities of D149Q and D149C for IPTG were decreased by ~4-fold, whereas those for D149T and D149E were decreased by ~13- and ~23-fold, respectively. Both S193A and S193C displayed IPTG binding affinities comparable to that of wild-type LacI (Figure 3 and Table 1).

To examine allosteric communication between DNA- and IPTG-binding sites, we quantified the release of DNA from the LacI·DNA complex in response to inducer. This assay determines the concentration of IPTG required to release 50% of the operator, which reflects the combined contributions of IPTG binding and the concomitant conformational change. For position 149, substitution with N, S, or A yielded essentially wild-type operator release values, whereas substitution with E, Q, T, and C shifted the midpoint of operator release. For D149E, which has most severe effect, $[IPTG]_{mid}$ for operator release was increased ~50-fold. D149T had a ~20-fold higher value, and values for both D149Q and D149C increased ~7-fold. For S193 single mutants, both S193A and S193C displayed operator release values comparable to that of wild-type LacI

Table 1: Thermodynamic Properties of Single Mutants[a]

	operator binding[b] K_d ($\times 10^{11}$ M)	with IPTG[c] K_d ($\times 10^{11}$ M)	IPTG binding[d] K_d ($\times 10^6$ M)	operator release[e] $[IPTG]_{mid}$ ($\times 10^6$ M)	induction ratio[f] $[IPTG]_{mid}/K_d$
WT LacI	2.2 ± 0.2	> 10000	1.5 ± 0.2	2.2 ± 0.2	1.5 ± 0.2
D149N	2.5 ± 0.2	> 10000	2.2 ± 0.2	2.5 ± 0.3	1.1 ± 0.2
D149E	3.4 ± 0.3	> 10000	**35 ± 4.0**	**110 ± 12**	3.2 ± 0.5
D149Q	2.5 ± 0.2	> 10000	**7.0 ± 0.8**	**16 ± 2.3**	2.3 ± 0.4
D149T	2.3 ± 0.2	> 10000	**19 ± 2.0**	**42 ± 3.6**	2.2 ± 0.2
D149S	3.5 ± 0.3	> 10000	3.2 ± 0.2	5.3 ± 0.5	1.6 ± 0.2
D149A	4.8 ± 0.3	> 10000	4.2 ± 0.3	4.6 ± 0.5	1.1 ± 0.2
D149C	5.0 ± 0.4	**> 1000**	**6.0 ± 0.7**	**14 ± 1.3**	2.3 ± 0.3
S193A	3.3 ± 0.3	> 10000	1.9 ± 0.2	4.2 ± 0.5	2.2 ± 0.3
S193C	3.1 ± 0.2	> 10000	2.4 ± 0.2	3.2 ± 0.4	1.3 ± 0.1

[a] Each value and standard deviation was generated by fitting at least three independently generated curves. Values in bold are those significantly different from that of the wild-type protein. [b] The equilibrium dissociation constants for the LacI·operator DNA complex were measured by nitrocellulose filter binding assays in FB buffer [0.01 M Tris-HCl (pH 7.4), 0.15 M KCl, 0.1 mM DTT, 0.1 mM EDTA, and 5% DMSO] with 100 μg/mL bovine serum albumin. The DNA concentration was 1.5×10^{-12} M. [c] The equilibrium dissociation constants for the LacI·operator DNA complex were measured as described in the presence of 1 mM IPTG. [d] The affinity of the protein for IPTG at pH 7.4 was measured by fluorescence assays in buffer containing 0.01 M Tris-HCl (pH 7.4) and 0.15 M KCl. The protein concentration was fixed at 1.5×10^{-7} M. [e] Operator release was monitored by nitrocellulose filter binding assays in FB buffer with 100 μg/mL bovine serum albumin. The DNA concentration was at least 10-fold below K_d, and the protein concentration was ~80% of maximal DNA binding. [f] The induction ratio is given by the ratio of $[IPTG]_{mid}$ to the K_d for inducer binding. Repressor variants with a ratio higher than that of the wild type have a potential block in allosteric communication.

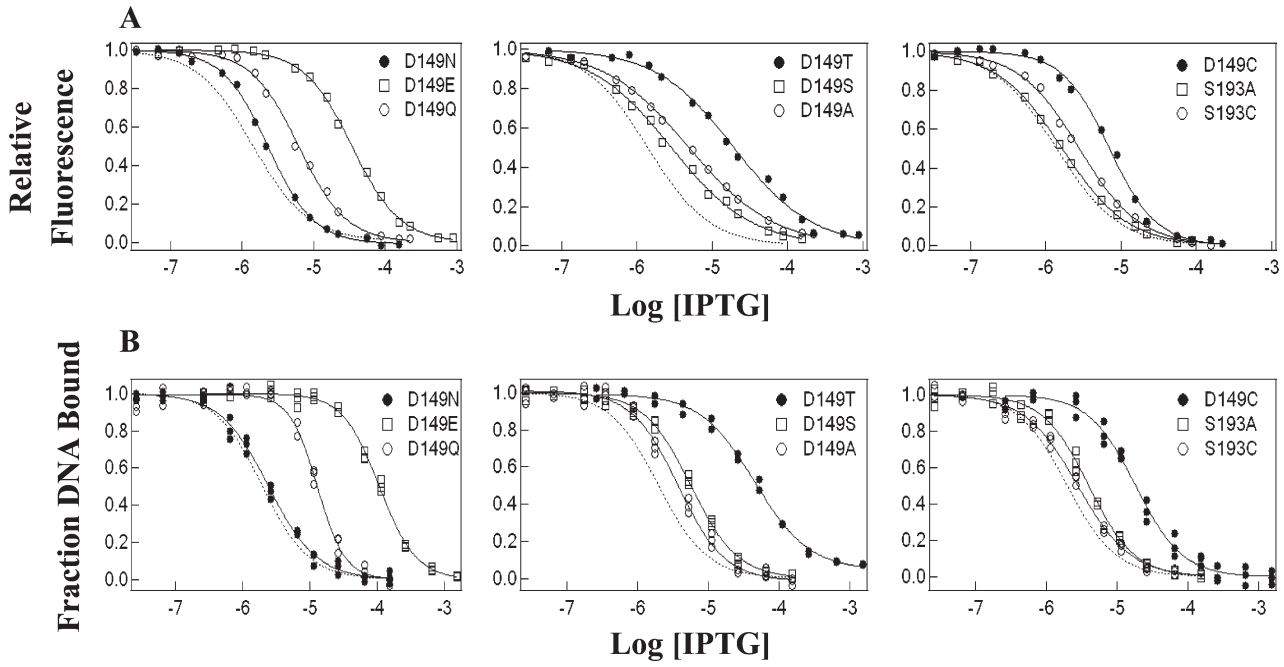

FIGURE 3: (A) IPTG binding curves and (B) operator release curves for wild-type LacI and single mutants. Wild-type LacI behavior is shown by a dotted line in each panel for the sake of comparison. IPTG binding assays were conducted in fluorescence buffer [0.01 M Tris-HCl (pH 7.4) and 0.15 M KCl] with a protein concentration of 1.5×10^{-7} M monomer, and operator release experiments were performed in FB buffer with 100 μg/mL bovine serum albumin with a DNA concentration of 1.5×10^{-12} M as described in Materials and Methods. Results from multiple experiments are listed in Table 1.

(Figure 3 and Table 1). Therefore, a subset of the D149 substitutions results in a diminished response to inducer binding with normal DNA affinity.

The alteration in IPTG release can derive from impaired IPTG binding or an impediment in the allosteric transition. The induction ratio, measured by the operator release midpoint ($[IPTG]_{mid}$) divided by the measured K_d for inducer binding, allows comparison between different LacI variants. Using this value, effects on allosteric communication can be distinguished from decreased IPTG binding affinity. For wild-type LacI, this ratio is ~1.5. The ratios for all mutants are within ~2-fold of that of wild-type LacI. Notice that although operator release $[IPTG]_{mid}$ values for D149E, D149Q, D149T, and D149C are larger than that for wild-type LacI, their IPTG binding affinities are weaker than that of wild-type LacI, resulting in induction ratios comparable to that of the wild type (Table 1). These data suggest that substitutions at residue 149 do not significantly impact LacI allostery, even when inducer binding affinity is affected.

Double Mutations at D149 and S193. Since single mutations at D149 or S193 did not significantly disrupt LacI allostery, two double mutants, D149A/S193A and D149C/S193C, were generated. The TMD simulation suggested that formation of hydrogen bonds between the side chains of D149 and S193 might be important to function (Figure 1C,D). Therefore, D149A/S193A was constructed to abolish the potential for hydrogen

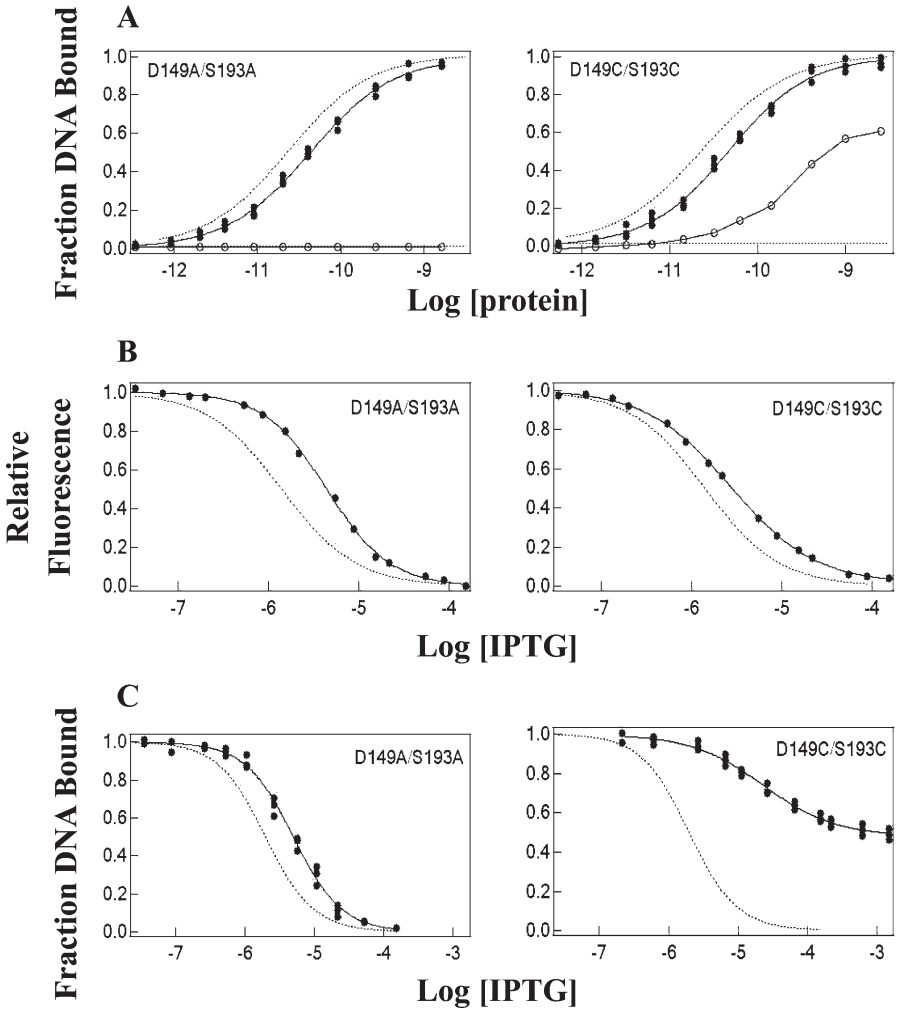

FIGURE 4: (A) Operator binding, (B) IPTG binding, and (C) operator release curves for wild-type LacI and double mutant proteins. Wild-type LacI behavior is shown by a dotted line for the sake of comparison. Operator binding and release assays were conducted in FB buffer with 100 μg/mL bovine serum albumin and a DNA concentration of 1.5×10^{-12} M, whereas IPTG binding experiments were conducted in fluorescence buffer with a protein concentration of 1.5×10^{-7} M monomer as described in Materials and Methods. For operator binding curves, the fraction DNA bound in the absence of IPTG is shown with filled circles and in the presence of 1 mM IPTG with empty circles. Results from multiple determinations are summarized in Table 2.

Table 2: Thermodynamic Properties of Double Mutants[a]

	operator binding[b] K_d ($\times 10^{11}$ M)	with IPTG[c] K_d ($\times 10^{11}$ M)	IPTG binding[d] K_d ($\times 10^6$ M)	operator release[e] $[IPTG]_{mid}$ ($\times 10^6$ M)	induction ratio[f] $[IPTG]_{mid}/K_d$
WT LacI	2.2 ± 0.2	>10000	1.5 ± 0.2	2.2 ± 0.2	1.5 ± 0.2
D149A/S193A	4.0 ± 0.3	>10000	4.2 ± 0.4	4.6 ± 0.4	1.1 ± 0.1
D149C/S193C	4.2 ± 0.5	**~100**	2.9 ± 0.2	**27 ± 2.1**	**9.3 ± 1.0**

[a] Each value and standard deviation was generated by fitting at least three independently generated curves. Values in bold are those significantly different from that of wild-type LacI. [b] The equilibrium dissociation constants for the LacI·operator DNA complex were measured by nitrocellulose filter binding assays in FB buffer [0.01 M Tris-HCl (pH 7.4), 0.15 M KCl, 0.1 mM DTT, 0.1 mM EDTA, and 5% DMSO] with 100 μg/mL bovine serum albumin. The DNA concentration was 1.5×10^{-12} M. [c] The equilibrium dissociation constants for the LacI·operator DNA complex in the presence of 1 mM IPTG. [d] The affinity of the protein for IPTG at pH 7.4 was measured by fluorescence in buffer containing 0.01 M Tris-HCl (pH 7.4) and 0.15 M KCl. The protein concentration was fixed at 1.5×10^{-7} M. [e] Operator release was monitored by nitrocellulose filter binding assays in FB buffer with 100 μg/mL bovine serum albumin. The DNA concentration was at least 10-fold below the K_d, and the protein concentration was ~80% of maximal DNA binding. [f] The induction ratio is given by the ratio of $[IPTG]_{mid}$ to the K_d for inducer binding. Repressors with a ratio higher than that of the wild type have a potential block in allosteric communication.

bond formation. Further, because the flexible loop that begins with D149 undergoes high mobility in the simulation, D149C/S193C was designed to constrain movement with a disulfide bond. In both operator- and IPTG-bound LacI structures, the distances between the C_α atoms of residues 149 and 193 are within a range favorable for disulfide formation as found for other systems (*28*).

Thermodynamic Properties of Double Mutants. The D149A/S193A double mutant displays operator and inducer binding affinities, as well as an $[IPTG]_{mid}$ value for operator release, within ~2-fold of wild-type values (Figure 4 and Table 2). The inducibility for D149A/S193A is close to that of the wild type, demonstrating that the ability to form hydrogen bonds between residues 149 and 193 is not critical for allosteric signal

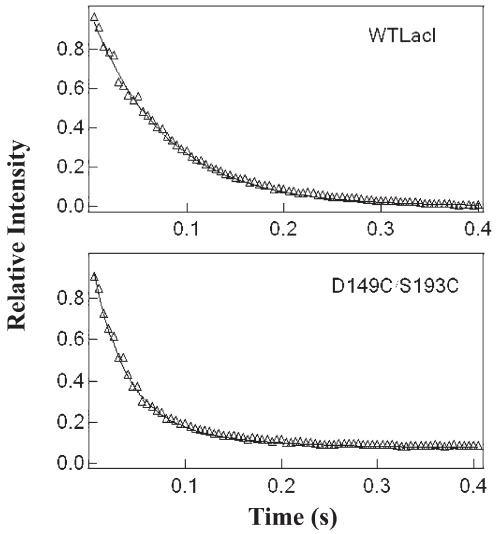

FIGURE 5: Measurement of association rate constants for binding of IPTG to wild-type LacI and D149C/S193C. The association rates for IPTG binding were determined by stopped-flow fluorescence spectroscopy as described in Materials and Methods. The excitation wavelength was 285 nm, and a cutoff filter (350 nm) was used to monitor the decrease in emission. For each repressor, protein (1.0×10^{-6} M) was mixed with multiple IPTG concentrations (from 0.05 to 0.2 mM) in fluorescence buffer. Shown are data from a single experiment using 0.05 mM IPTG. Results from the complete analysis are summarized in Table 3.

transduction. Interestingly, the double mutant D149C/S193C has operator binding affinity comparable to that of wild-type LacI in the absence of IPTG, whereas in the presence of 1 mM IPTG, this mutant still binds to operator, reflecting decreased sensitivity to inducer binding (Figure 4 and Table 2). This double-cysteine mutant exhibited IPTG binding affinity within ~2-fold of that of wild-type LacI. Resistance of D149C/S193C to release of operator by inducer binding was confirmed by the operator release assay, with a >12-fold increased $[IPTG]_{mid}$ value; further, the induction ratio is ~6-fold higher than that for wild-type LacI (Table 2).

To explore whether reciprocal behavior could be measured for the impact of operator on IPTG binding, [^{14}C]IPTG binding was measured in the assay buffer for operator binding. The retention of IPTG at protein concentrations just above the protein·DNA K_d and stoichiometric operator DNA was diminished by ~2-fold for D149C/S193C compared to that of wild-type LacI (data not shown), consistent with expectations from DNA binding results. These distinct properties of D149C/S193C meet the criteria for an allosteric LacI mutant, and flexibility for movement in the region encompassed by D149 and/or S193 appears to be critical for allosteric regulation.

Kinetic Measurements of Repressor−IPTG Association. To ensure that the differences for D149C/S193C were not kinetic in origin, association of the wild type and D149C/S193C with IPTG and dissociation from operator were measured. The IPTG association rate constant for the wild-type protein is 1.1×10^5 M^{-1} s^{-1} at pH 7.4, consistent with data from previous work (*24*, *29*, *30*). The value for D149C/S193C is within ~2-fold of that for wild-type LacI (Figure 5 and Table 3). Dissociation rate constants were derived from the plot of k_{assoc} versus the concentration of IPTG, and the D149C/S193C value was ~3-fold greater than that for wild-type LacI. Thus, the disulfide bond between residues 149 and 193 does not substantially impact the rate constants for binding of D149C/S193C to IPTG. The equilibrium constant for each reaction computed from the corresponding rate constants was comparable within ~2-fold to the value for the K_d determined directly from fluorescence titration (Table 3).

Kinetic Measurements of Repressor−Operator Dissociation. The operator dissociation rate constants were measured by adding unlabeled operator DNA to trap released repressor (*25*). The dissociation rate constants for wild-type LacI and D149C/S193C measured under same conditions were essentially identical (Figure 6 and Table 3). These data demonstrate that introducing a disulfide bond between residues 149 and 193 does not significantly influence kinetics for repressor−operator dissociation.

Determination of the Number of Cysteines. To assess directly the formation of the disulfide bond in D149C/S193C, we determined the number of free cysteines per monomer in this double mutant by Ellman's reaction in 6 M urea to provide a quantitative measure of available thiols (*26*, *27*). The results demonstrate that the ratio of thionitrobenzoate anion produced to monomer concentration is 2.9 ± 0.1 for wild-type LacI, indicating that each monomer exhibits the expected 3 free cysteines (residues 107, 140, and 281) (*31*). For the double mutant D149C/S193C, 4.0 ± 0.1 free cysteines are detected in the native monomeric state, suggesting there is a mixture of the oxidized and reduced forms of the protein present in solution. Following treatment with DTT and rapid removal by a desalting column, 4.6 ± 0.1 free cysteines are detected, indicating more reduced D149C/S193C is obtained. Also, the D149C/S193C mutant can be pushed toward the oxidized state by removing DTT through a desalting column and dialyzing in air-bubbled buffer. Under this condition, 3.3 ± 0.1 free cysteines per monomer are detected.

Since D149C/S193C with more and less oxidation can be obtained experimentally, the impact of the varied extent of disulfide bond formation was further examined. As controls, the thermodynamic properties of wild-type protein produced under the same conditions for both oxidization and reduction were also examined. The operator binding affinities for oxidized- and reduced-state D149C/S193C are decreased compared to that of the untreated protein, consistent with results for wild-type LacI under the same conditions (Figure 7 and Table 4). In the presence of a high concentration of 1 mM IPTG, D149C/S193C in both states can still bind to operator DNA with higher affinity than wild-type LacI (Figure 7 and Table 4), with the oxidized protein binding ~9-fold more tightly. IPTG binding affinities for oxidized and reduced D149C/S193C are comparable to those of the untreated double mutant and wild-type LacI. Importantly, the operator release data demonstrate that the oxidized and reduced forms of D149C/S193C have distinct sensitivity to IPTG, reflected in the ~10-fold difference between their $[IPTG]_{mid}$ values (Table 4). Therefore, the induction ratios for oxidized and reduced D149C/S193C are >10-fold different. The difference in response to IPTG binding between the oxidized and reduced forms of D149C/S193C confirms that the disulfide bond introduced impedes allosteric signal transduction within the LacI structure.

DISCUSSION

Despite broad exploration of LacI as a regulatory protein, neither D149 nor S193 has been targeted for biochemical analysis of substitutions. Previous phenotypic analysis demonstrated that alterations at these sites result in proteins insensitive to IPTG

Table 3: Kinetic Constants for Ligand Binding

	IPTG				DNA
	k_{assoc}[a] ($\times 10^{-5}$ M^{-1} s^{-1})	k_{dissoc}[b] (s^{-1})	calcd k_{dissoc}/k_{assoc} ($\times 10^{6}$ M)	K_d[c] ($\times 10^{6}$ M)	k_{dissoc}[d] ($\times 10^{3}$ s^{-1})
WT LacI	1.1 ± 0.1	0.3 ± 0.1	2.7 ± 0.3	1.4 ± 0.2	5.4 ± 0.3
D149C/S193C	2.3 ± 0.2	1.0 ± 0.3	4.4 ± 0.3	2.5 ± 0.2	5.0 ± 0.2

[a] The association rate constants for IPTG binding were obtained by stopped-flow experiments at 25 °C in fluorescence buffer [0.01 M Tris-HCl (pH 7.4) and 0.15 M KCl]. Error values represent the standard deviation for a minimum of three measurements. [b] Values were calculated from the intercept of the plot of k_{obsd} vs IPTG concentration. [c] Values were measured by fluorescence titration in fluorescence buffer. [d] The dissociation rate constants for dissociation of repressors from operator DNA utilized a nitrocellulose filter binding assay in FB buffer [0.01 M Tris-HCl (pH 7.4), 0.15 M KCl, 0.1 mM DTT, 0.1 mM EDTA, and 5% DMSO] with 100 μg/mL bovine serum albumin. The protein concentration was 1.8×10^{-11} M, and the labeled DNA concentration was 3.6×10^{-11} M. Unlabeled DNA was at 90-fold excess over labeled DNA.

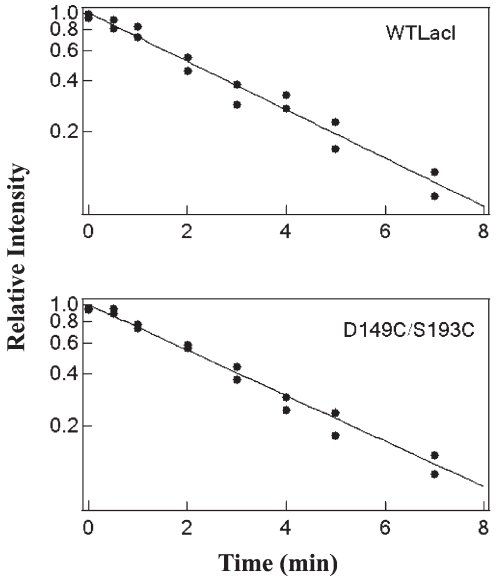

FIGURE 6: Determination of dissociation rate constants for dissociation of operator DNA from repressor. The *Y*-axis is shown in exponential format for ease of comparison. This measurement was conducted by nitrocellulose filter binding in FB buffer with 100 μg/mL bovine serum albumin as described in Materials and Methods. Repressor (1.8×10^{-11} M) and ^{32}P-labeled operator (3.6×10^{-11} M) were equilibrated for 15 min before a 90-fold excess of unlabeled DNA was added to the mixture at time zero. Samples were taken at time intervals for analysis. The equilibrium value measured at 2 h was subtracted from the data at each time point to determine the extent of release, and values were normalized relative to binding at time zero. The dissociation rate constants reported in Table 3 were determined by fitting the data to a single-exponential model.

binding (*14*). However, since D149 is among the amino acids that have direct contact with inducer IPTG, this phenotype could be caused by either diminished IPTG binding affinity or impaired allosteric transition. In this study, a series of D149 and S193 point mutations were generated to examine the effects of different amino acid side chains on function. The induction ratios for the D149 single mutants are within ~2-fold of that for the wild-type protein, suggesting that coupling between inducer binding and the allosteric conformational change is not altered. In addition, both S193 single mutants, S193A and S193C, display wild-type properties. The data for single substitutions at either D149 or S193 demonstrate that substitutions at these sites either exert a minimal effect on LacI binding properties or alter both inducer binding affinity and operator release, without significantly affecting the allosteric transition (i.e., there is no impact on the induction ratio).

In different ligand-bound structures, distinct interactions are observed between D149 or S193 and other surrounding amino acids. For example, the IPTG-bound LacI structure evinces at least one hydrogen bond between the R197 polypeptide backbone and the S193 backbone or side chain (*8*). In the operator-bound conformation, backbone hydrogen bonds are present between D149 and L128/Y126 (*16*). The double mutant D149A/S193A was designed for exploration of the importance of hydrogen bond formation by precluding the side chain contribution at these positions. Interestingly, the double-alanine substitution does not affect binding properties of LacI, with operator binding and release properties being similar to those of the wild-type protein. Loss of hydrogen bond capacity may be compensated by the proximal alanine−alanine hydrophobic interaction to promote allosteric signaling.

D149 is at the start of a loop (residues 149−156), for which the flexibility was postulated to be a key factor in the structural transition (*18*). The TMD results for LacI indicate that the mobility in this loop accompanies the early steps in propagating the inducer binding signal from the binding pocket to the DNA-binding site (*18*). To reduce flexibility within this region, residues that could form a disulfide bond were introduced by converting residues 149 and 193 to cysteines. This double-cysteine mutant indeed forms a disulfide bond between residues 149 and 193, and this variant binds with wild-type affinity to both operator and inducer. However, the D149C/S193C protein exhibits a diminished impact of inducer binding on operator affinity compared to wild-type LacI and has an induction ratio of ~9, more than 6-fold greater than those of wild-type LacI and other mutants, including the single substitutions D149C and S193C.

To confirm that disulfide bond formation was the basis for the change in induction ratio, D149C/S193C was exposed to conditions designed to "push" toward either the oxidized or reduced state. Oxidized D149C/S193C displays an even higher induction ratio (~16) than the protein as purified from bacterial cells (~9), whereas the reduced-state double mutant displays an induction ratio near that for wild-type LacI. This substantial difference between oxidized and reduced D149C/S193C is consistent with the hypothesis that flexibility in the 149−156 region is necessary for signal transmission at the initial stage of the allosteric transition in response to inducer binding.

Limited motions at position 149 or 193 in the double-cysteine mutant D149C/S193C may influence various interactions with other residues. The TMD simulation indicates that D149 also forms a hydrogen bond with the backbone of F161, just before the flexible loop is stabilized by interaction with S193 (*18*). F161 is located in the center of a hydrophobic cluster that also experiences a high degree of mobility during the simulation. If interaction with F161 is impaired, the function of the entire hydrophobic cluster during the allosteric transition may be compromised. Further, the intermediate state of TMD

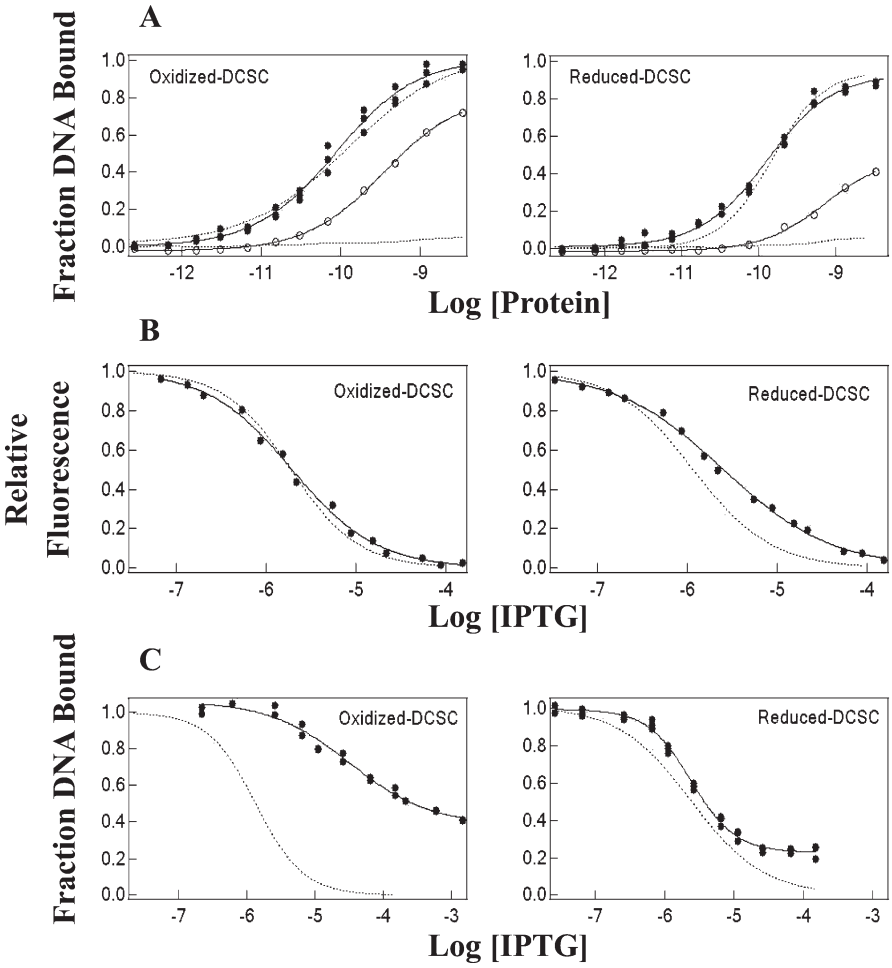

FIGURE 7: (A) DNA binding, (B) IPTG binding, and (C) operator release curves for wild-type LacI and D149C/S193C exposed to oxidizing and reducing conditions. Wild-type LacI behavior for the oxidized and reduced states is represented by the dotted line with data shown for oxidized and reduced D149C/S193C. Operator binding and release assays were conducted in FB buffer with 100 μg/mL bovine serum albumin with a DNA concentration of 1.5×10^{-12} M and IPTG binding experiments in fluorescence buffer with a protein concentration of 1.5×10^{-7} M monomer as described in Materials and Methods. The curves were generated by fitting the data in Igor Pro. Results from multiple experiments are listed in Table 4.

Table 4: Thermodynamic Properties of Oxidized- and Reduced-State Repressors[a]

	operator binding[b] K_d ($\times 10^{11}$ M)	with IPTG[c] K_d ($\times 10^{11}$ M)	IPTG binding[d] K_d ($\times 10^6$ M)	operator release[e] $[IPTG]_{mid}$ ($\times 10^6$ M)	induction ratio[f] $[IPTG]_{mid}/K_d$
WT LacI (O[g])	13 ± 2.0	> 10000	1.9 ± 0.2	1.7 ± 0.2	0.9 ± 0.1
WT LacI (R[h])	16 ± 1.0	> 10000	1.2 ± 0.1	2.3 ± 0.4	1.9 ± 0.2
D149C/S193C (O)	10 ± 1.0	**~75**	2.0 ± 0.2	**31 ± 2.7**	**16 ± 2.0**
D149C/S193C (R)	15 ± 1.6	**~650**	2.6 ± 0.2	3.0 ± 0.2	1.2 ± 0.1

[a] Each value and standard deviation was generated by fitting at least three independently generated curves by Igor Pro. Values in bold are those significantly different from that of wild-type LacI. [b] The equilibrium dissociation constants for the LacI·operator DNA complex were measured by nitrocellulose filter binding assays in FB buffer [0.01 M Tris-HCl (pH 7.4), 0.15 M KCl, 0.1 mM DTT, 0.1 mM EDTA, and 5% DMSO] with 100 μg/mL bovine serum albumin. The DNA concentration was 1.5×10^{-12} M. [c] The equilibrium dissociation constants for the LacI·operator DNA complex in the presence of 1 mM IPTG. [d] The affinity of the protein for IPTG at pH 7.4 was measured by fluorescence in buffer containing 0.01 M Tris-HCl (pH 7.4) and 0.15 M KCl. The protein concentration was fixed at 1.5×10^{-7} M. [e] Operator release was monitored by nitrocellulose filter binding assays in FB buffer with 100 μg/mL bovine serum albumin. The DNA concentration was at least 10-fold below K_d, and the protein concentration was ~80% of maximal DNA binding. [f] The induction ratio is given by the ratio of $[IPTG]_{mid}$ to K_d for inducer binding. Repressors with a ratio higher than that of the wild type have a potential block in allosteric communication. [g] Oxidized-state repressor. [h] Reduced-state repressor.

simulation reveals the side chain of D149 transiently flips toward residue N125, which provides the opportunity to form a hydrogen bond between side chains of D149 and N125 during the process of transmitting the IPTG binding signal to the DNA-binding domain (*18*). However, an interaction between residues 149 and 125 is not present in the extreme DNA- and IPTG-bound conformations (*8*, *16*).

For S193, a hydrogen bond between side chains of residues S193 and R197 is observed in the DNA-bound structure (*16*). During TMD simulation, this side chain bond breaks, and new hydrogen bonds are generated between the backbone of R197 and the side chain or backbone of S193 (*18*). However, the interaction between these side chains is not restored in the inducer-bound structure, indicating its importance only in the

DNA-bound conformation. Interactions between D149 or S193 and other amino acids may contribute to allosteric regulation in LacI, but the double-cysteine mutant D149C/S193C limits the movement of these residues, which may consequently affect the conformational change. Which of these interactions individually or in combination is crucial for the structural shifts that are responsible for allostery cannot be discerned from these data. However, the importance of flexibility in this region is clearly evident.

Protein flexibility appears to play a general role in propagating a signal from a localized perturbation (e.g., ligand binding or point mutation), allowing long-range communication that is fundamental to many protein functions (e.g., refs (*32*−*36*)). In an analysis of more than 50 pairs of protein structures, each in two different states, structural motion carries information over long distances in both sequence and space (*37*). Interestingly, the observed motions favor residues located in the less constrained loops and at the protein surface, and ~2-fold greater motion is observed in allosteric proteins (*37*). A very recent model that describes allosteric motion for multiple proteins suggests that contact rearrangement is key to the quaternary changes that occur in LacI (*38*), consistent with the results reported in this study.

In LacI, substitution of other residues in this solvent-exposed flexible loop that encompasses amino acids 149−156 results in altered inducer and operator binding affinities (*23*). For example, despite induction ratios similar to that of wild-type LacI, the two mutations L148F and S151P are an "opposite" pair: L148F exhibits lowered affinity for operator and increased affinity for IPTG, whereas S151P has enhanced operator binding and diminished IPTG binding affinity (*23*). These results are consistent with a role for this flexible loop in regulating LacI allosteric equilibrium. Thus, residues in this flexible loop appear to make a key contribution to allosteric regulation, perhaps by impacting the range and nature of structural states available to the protein.

Overall, the mutants described herein provide specific insight into the role of D149 and S193 in LacI allosteric response. The experimental results demonstrate that impeding mobility in the D149/S193 region by disulfide bond formation interrupts the transmission of the allosteric signal from the IPTG-binding pocket to the DNA-binding domain without significantly affecting IPTG and operator binding. Integration of biochemical examination of LacI variants with structural analysis and computational simulation provides an important avenue for completing our understanding of allosteric communication within LacI. This work provides a direct demonstration of the general utility of coupling experimental work with computational simulation for identifying regions of a protein crucial for function.

ACKNOWLEDGMENT

We thank members of the Matthews laboratory for helpful discussion and suggestions on experiments and Dr. Liskin Swint-Kruse for sage advice and critical reading of the manuscript.

REFERENCES

1. Goodey, N. M., and Benkovic, S. J. (2008) Allosteric regulation and catalysis emerge via a common route. *Nat. Chem. Biol. 4*, 474–482.
2. Gunasekaran, K., Ma, B., and Nussinov, R. (2004) Is allostery an intrinsic property of *all* dynamic proteins?. *Proteins 57*, 433–443.
3. Jacob, F., and Monod, J. (1961) Genetic regulatory mechanisms in the synthesis of proteins. *J. Mol. Biol. 3*, 318–356.
4. Matthews, K. S., and Nichols, J. C. (1998) Lactose repressor protein: Functional properties and structure. *Prog. Nucleic Acid Res. Mol. Biol. 58*, 127–164.
5. Gilbert, W., and Müller-Hill, B. (1967) The *lac* operator is DNA. *Proc. Natl. Acad. Sci. U.S.A. 58*, 2415–2421.
6. Chuprina, V. P., Rullmann, J. A. C., Lamerichs, R. M. J. N., van Boom, J. H., Boelens, R., and Kaptein, R. (1993) Structure of the complex of *lac* repressor headpiece and an 11 base-pair half-operator determined by nuclear magnetic resonance spectroscopy and restrained molecular dynamics. *J. Mol. Biol. 234*, 446–462.
7. Friedman, A. M., Fischmann, T. O., and Steitz, T. A. (1995) Crystal structure of *lac* repressor core tetramer and its implications for DNA looping. *Science 268*, 1721–1727.
8. Lewis, M., Chang, G., Horton, N. C., Kercher, M. A., Pace, H. C., Schumacher, M. A., Brennan, R. G., and Lu, P. (1996) Crystal structure of the lactose operon repressor and its complexes with DNA and inducer. *Science 271*, 1247–1254.
9. Chen, J., and Matthews, K. S. (1992) Deletion of lactose repressor carboxyl-terminal domain affects tetramer formation. *J. Biol. Chem. 267*, 13843–13850.
10. Felder, C. B., Graul, R. C., Lee, A. Y., Merkle, H. P., and Sadee, W. (1999) The Venus flytrap of periplasmic binding proteins: An ancient protein module present in multiple drug receptors. *AAPS J. 1*, 7–26.
11. Quiocho, F. A., and Ledvina, P. S. (1996) Atomic structure and specificity of bacterial periplasmic receptors for active transport and chemotaxis: Variation of common themes. *Mol. Microbiol. 20*, 17–25.
12. Acher, F. C., and Bertrand, H. O. (2005) Amino acid recognition by Venus flytrap domains is encoded in an 8-residue motif. *Biopolymers 80*, 357–366.
13. Miller, J. H. (1979) Genetic studies of the *lac* repressor XI. On aspects of *lac* repressor structure suggested by genetic experiments. *J. Mol. Biol. 131*, 249–258.
14. Suckow, J., Markiewicz, P., Kleina, L. G., Miller, J., Kisters-Woike, B., and Müller-Hill, B. (1996) Genetic studies of the Lac repressor XV: 4000 single amino acid substitutions and analysis of the resulting phenotypes on the basis of the protein structure. *J. Mol. Biol. 261*, 509–523.
15. Matthews, K. S., Falcon, C. M., and Swint-Kruse, L. (2000) Relieving repression. *Nat. Struct. Biol. 7*, 184–187.
16. Bell, C. E., and Lewis, M. (2000) A closer view of the conformation of the Lac repressor bound to operator. *Nat. Struct. Biol. 7*, 209–214.
17. Pace, H. C., Kercher, M. A., Lu, P., Markiewicz, P., Miller, J. H., Chang, G., and Lewis, M. (1997) *Lac* repressor genetic map in real space. *Trends Biochem. Sci. 22*, 334–339.
18. Flynn, T. C., Swint-Kruse, L., Kong, Y., Booth, C., Matthews, K. S., and Ma, J. (2003) Allosteric transition pathways in the lactose repressor protein core domains: Asymmetric motions in a homodimer. *Protein Sci. 12*, 2523–2541.
19. Wycuff, D. R., and Matthews, K. S. (2000) Generation of an AraC-*ara*BAD promoter-regulated T7 expression system. *Anal. Biochem. 277*, 67–73.
20. Falcon, C. M., and Matthews, K. S. (1999) Glycine insertion in the hinge region of lactose repressor protein alters DNA binding. *J. Biol. Chem. 274*, 30849–30857.
21. O′Gorman, R. B., Rosenberg, J. M., Kallai, O. B., Dickerson, R. E., Itakura, K., Riggs, A. D., and Matthews, K. S. (1980) Equilibrium binding of inducer to *lac* repressor·operator DNA complex. J. Biol. Chem. 255, 10107–10114.
22. Laiken, S. L., Gross, C. A., and von Hippel, P. H. (1972) Equilibrium and kinetic studies of *Escherichia coli lac* repressor-inducer interactions. *J. Mol. Biol. 66*, 143–155.
23. Swint-Kruse, L., Zhan, H., Fairbanks, B. M., Maheshwari, A., and Matthews, K. S. (2003) Perturbation from a distance: Mutations that alter LacI function through long-range effects. *Biochemistry 42*, 14004–14016.
24. Friedman, B. E., Olson, J. S., and Matthews, K. S. (1977) Interaction of *lac* repressor with inducer. Kinetic and equilibrium measurements. *J. Mol. Biol. 111*, 27–39.
25. Whitson, P. A., and Matthews, K. S. (1986) Dissociation of the lactose repressor-operator DNA complex: Effects of size and sequence context of operator-containing DNA. *Biochemistry 25*, 3845–3852.
26. Ellman, G. L. (1959) Tissue sulfhydryl groups. *Arch. Biochem. Biophys. 82*, 70–77.
27. Riddles, P. W., Blakeley, R. L., and Zerner, B. (1983) Reassessment of Ellman′s reagent. *Methods Enzymol. 91*, 49–60.

28. Tiebel, B., Aung-Hilbrich, L. M., Schnappinger, D., and Hillen, W. (1998) Conformational changes necessary for gene regulation by Tet repressor assayed by reversible disulfide bond formation. *EMBO J. 17*, 5112–5119.
29. Chakerian, A. E., Olson, J. S., and Matthews, K. S. (1987) Thermodynamic analysis of inducer binding to the lactose repressor protein: Contributions of galactosyl hydroxyl groups and β substituents. *Biochemistry 26*, 7250–7255.
30. Xu, H., Moraitis, M., Reedstrom, R. J., and Matthews, K. S. (1998) Kinetic and thermodynamic studies of purine repressor binding to corepressor and operator DNA. *J. Biol. Chem. 273*, 8958–8964.
31. Yang, D. S., and Matthews, K. S. (1976) Lactose repressor protein reaction with 2-chloromercuri-4-nitrophenol. *J. Mol. Biol. 103*, 433–437.
32. Clarkson, M. W., and Lee, A. L. (2004) Long-range dynamic effects of point mutations propagate through side chains in the serine protease inhibitor eglin c. *Biochemistry 43*, 12448–12458.
33. Yu, E. W., and Koshland, D. E.Jr. (2001) Propagating conformational changes over long (and short) distances in proteins. *Proc. Natl. Acad. Sci. U.S.A. 98*, 9517–9520.
34. Shaw, D., Wang, S. M., Villaseñor, A. G., Tsing, S., Walter, D., Browner, M. F., Barnett, J., and Kuglstatter, A. (2008) The crystal structure of JNK2 reveals conformational flexibility in the MAP kinase insert and indicates its involvement in the regulation of catalytic activity. *J. Mol. Biol. 383*, 885–893.
35. Dodson, G., and Verma, C. S. (2006) Protein flexibility: Its role in structure and mechanism revealed by molecular simulations. *Cell. Mol. Life Sci. 63*, 207–219.
36. Benson, N. C., and Daggett, V. (2008) Dynameomics: Large-scale assessment of native protein flexibility. *Protein Sci. 17*, 2038–2050.
37. Daily, M. D., and Gray, J. J. (2007) Local motions in a benchmark of allosteric proteins. *Proteins 67*, 385–399.
38. Daily, M. D., and Gray, J. J. (2009) Allosteric communication occurs via networks of tertiary and quaternary motions in proteins. *PLoS Comput. Biol. 5*, e1000293.